ELSEVIER

Physics of the Earth and Planetary Interiors 129 (2002) 265–282

PHYSICS OF THE EARTH AND PLANETARY INTERIORS

www.elsevier.com/locate/pepi

Grain size in the lower mantle: constraints from numerical modeling of grain growth in two-phase systems

V.S. Solomatov [a,*], R. El-Khozondar [a], V. Tikare [b]

[a] *Department of Physics, New Mexico State University, P.O. Box 30001, Las Cruces, NM 88003, USA*
[b] *Materials Modeling and Simulation, Sandia National Laboratories, MS 1405, Albuquerque, NM 87185, USA*

Received 15 August 2000; received in revised form 22 August 2001; accepted 17 October 2001

Abstract

The lower mantle is believed to deform in the grain size-sensitive creep regime. Analysis of physical processes in the convective mantle suggests that the grain size is probably very small immediately after the phase transformations at 660 km depth and is controlled by subsequent grain growth. It was proposed that the microstructural evolution of two-phase aggregates eventually reaches an asymptotic regime in which grain growth in both phases is coupled due to Zener pinning and obeys a power-law scaling relationship $d \propto t^{1/n}$. We performed Monte Carlo simulations for a particular case in which grain growth is controlled by diffusion along grain boundaries ($n = 4$) and found a good agreement with theoretical predictions. On geological time scales the grain size of (Mg, Fe)-perovskite is controlled by Ostwald ripening of magnesiowüstite and Ca-perovskite. However, the physical parameters are poorly constrained and the grain size remains highly uncertain. If the rate-limiting process is silicon diffusion, the coarsening exponent is likely to be $n = 3$ and the grain size is likely to be 100–1000 μm.

Keywords: Grain size; Lower mantle; Monte Carlo simulations

1. Introduction

The lack of anisotropy in the lower mantle of the Earth (Meade et al., 1995) suggests that deformation in this region is controlled by diffusion creep or superplasticity (Karato et al., 1995). This implies that the viscosity, η, of the lower mantle depends on the grain size, d. Usually this dependence is described as a power-law function $\eta \sim d^m$. The value of the constant m is between 2 and 3 (Karato and Wu, 1993) although in the superplastic regime it can take values in a broader range (Nieh et al., 1997).

Why is this important? First of all, this means that constraints on temperature and pressure alone are insufficient to calculate the viscosity of the lower mantle. We need constraints on the grain size as well. Secondly, variations in the grain size can cause variations in the viscosity, which are comparable to or even larger than those due to temperature and pressure. In extreme cases, variations in the grain size can be so large that hot regions can be more viscous than cold regions because of enhanced grain growth (Solomatov, 1996; Karato, 1997). Grain size variations are important for virtually all problems of geodynamics, where variable viscosity matters, including chemical mixing (Manga, 1996), thermal

* Corresponding author. Fax: +1-505-646-1934.
E-mail addresses: slava@nmsu.edu (V.S. Solomatov), relkhozo@nmsu.edu (R. El-Khozondar), vtikare@sandia.gov (V. Tikare).

0031-9201/02/$ – see front matter
PII: S0031-9201(01)00295-3

evolution (Christensen, 1984), the regime of mantle convection (Solomatov and Moresi, 1997), the gravity of the planet (King, 1995) and strain localization (Kameyama et al., 1997; Braun et al., 1999).

Although grain growth in perovskite–magnesiowüstite system under lower mantle conditions has been investigated by Yamazaki et al. (1996), an unusually sluggish growth observed in these experiments cannot be easily reconciled with either theoretical models or laboratory data for other materials. If Yamazaki et al.'s (1996) results were correct, then grain growth would have a very mild effect on mantle dynamics and evolution. On the other hand, "classical" grain growth can dramatically affect mantle dynamics and evolution (Solomatov, 1996, 2001). The goal of this study is to review the physical mechanisms controlling the grain size in the lower mantle, discuss possible explanations of Yamazaki et al.'s (1996) results and suggest some constraints on the grain size in the lower mantle based on previous experimental and theoretical results as well as our own numerical simulations.

2. Grain size upon the phase transformations at 660 km depth

What controls the grain size in the lower mantle? If the viscosity were dominated by steady-state dislocation creep, then the grain size would be controlled by dynamic recrystallization. In this case, the grain size is a function of shear stress. In the diffusion creep regime, the grains do not reach the critical size at which grain-size reduction processes become efficient (such as nucleation and subgrain rotation, Derby and Ashby, 1987; Shimizu, 1998). In this case, the grain size is controlled by phase transformations and grain growth.

Phase transformations in the upper mantle can be considered separately for the olivine and pyroxene subsystems (e.g. Ita and Stixrude, 1993). At 660 km depth, the olivine phase, spinel, transforms to (Mg, Fe)SiO_3-perovskite and (Mg, Fe)O-magnesiowüstite (e.g. Irifune and Ringwood, 1987b; Ito and Takahashi, 1987). In the pyroxene subsystem, majorite garnet transforms to (Mg, Fe)SiO_3- and $CaSiO_3$-perovskite at about the same depth (Irifune and Ringwood, 1987b; Ito and Takahashi, 1987) although the transition is spread out over a larger depth range. Another phase could be Al-perovskite but it dissolves in (Mg, Fe)SiO_3-perovskite and does not form a separate phase (Weng et al., 1982; Irifune and Ringwood, 1987a; Irifune, 1994; Kubo and Akaogi, 2000). These transformations produce three phases: about 75% of (Mg, Fe)SiO_3-perovskite, 15% of magnesiowüstite, and 10% of $CaSiO_3$-perovskite (Ita and Stixrude, 1993; Jackson and Rigden, 1998). The original grains of spinel (olivine subsystem) and garnet (pyroxene subsystem) are likely to form two domains corresponding to these two phases: spinel grains would form two-phase domains consisting of (Mg, Fe)SiO_3-perovskite and magnesiowüstite grains while the garnet grains would form two-phase domains consisting of (Mg, Fe)SiO_3- and $CaSiO_3$-perovskite. The sizes of these two domains are probably on the scale of the grain size typical for the upper mantle, which is in the order of 10^{-4} to 10^{-2} m (Karato, 1984, 1989; Karato and Wu, 1993).

How big are the grains in each of these two-phase domains? The transformation in the olivine subsystem is an eutectoid-type transformation which produces extremely thin lamellae of alternating perovskite and magnesiowüstite with the spacing of $<0.1\,\mu$m (Poirier et al., 1986; Ito and Sato, 1991; Wang et al., 1997; Martinez et al., 1997; Kubo et al., 2000). The lamellar spacing in these type of transformations is inversely proportional to the metastable overshoot, that is, the difference between the pressure at which the transformation actually occurs and the pressure for equilibrium transformation (Sundquist, 1968; Hillert, 1972; Puls and Kirkaldy, 1972; Livingston and Cahn, 1974). In the simplest form, it can be written as

$$s \approx \frac{4\sigma\lambda T_0}{\rho \Delta H \Delta P} \tag{1}$$

where σ is the interface energy, λ the Clapeyron slope, T_0 the equilibrium eutectic temperature, ΔH the enthalpy change upon the phase transformation, and ΔP is the overpressure. The typical values of these parameters are $\sigma \sim 1\,\mathrm{J\,m^{-2}}$ (Cooper and Kohlstedt, 1982), $|\lambda| \sim 3\,\mathrm{MPa\,K^{-1}}$ (Ito and Takahashi, 1989; Ito et al., 1990), $T_0 \sim 2000\,\mathrm{K}$, $\rho \sim 4 \times 10^3\,\mathrm{kg\,m^{-3}}$, $\Delta\rho/\rho \sim 0.1$ (Anderson, 1989) and $\Delta H = \lambda \Delta\rho T_0/\rho^2 \sim 10^5\,\mathrm{J\,kg^{-1}}$. If we assume that the overpressure is in the order of the nucleation barrier which is probably about several kilometers (Rubie and Ross, 1994; Solomatov and Stevenson, 1994; Daessler et al.,

1996; Riedel and Karato, 1997) and roughly the same as the overpressure used in the laboratory experiments, then the laminar spacing is about $s \sim 0.1\,\mu m$. This is similar to that observed in the laboratory experiments.

It is possible that the transformation could propagate back towards the equilibrium phase boundary and stop at such distance from the equilibrium that the growth rate is equal to the convective velocity (Solomatov and Stevenson, 1993). To calculate spacing in this case, we can use the relationship between the spacing s, the growth rate G and the overpressure ΔP. For volume diffusion, it can be written as (Sundquist, 1968; Hillert, 1972; Puls and Kirkaldy, 1972; Livingston and Cahn, 1974)

$$G \sim \frac{\alpha}{\lambda}\frac{D\Delta P}{s} \tag{2}$$

where α is a coefficient found from the phase diagram (usually in the order of $\alpha \sim T_0^{-1}$), and $D \sim 10^{-18}\,m^2\,s^{-1}$ is the coefficient of volume diffusion (Yamazaki et al., 2000). Requiring that G is in the order of convective velocities, $10^{-9}\,m\,s^{-1}$, and solving Eqs. (1) and (2) for ΔP and s, we obtain even smaller values, $s \sim 0.01\,\mu m$.

The grain size is more difficult to estimate for pyroxene subsystem because the kinetics of phase transformations in this subsystem is poorly understood (Hogrefe et al., 1994). As in the spinel–perovskite transformation, the phase transformation at the bottom of the upper mantle produces two phases and, thus the transformation is likely to be characterized by long-range diffusion and a very fine structure (see also Rubie, 1993; Porter and Easterling, 1997).

The grain size after degeneration of the lamellar structure depends on the rates of various competing kinetic processes (Graham and Kraft, 1966; Weatherly, 1975; Chattopadhyay and Sellars, 1982; Bartholomeusz and Wert, 1994; Whiting and Tsakiropoulos, 1997; Sharma et al., 2000). The grain size of degenerated lamellae is usually several times larger than the initial lamellar spacing. This implies that immediately after the phase transformations at 660 km depth, the grain size is unlikely to be bigger than about 1 μm. As the convective flow carries the material below the 660 km depth, the grains can grow via several mechanisms described as follows.

3. How fast do grains grow after the phase transformations?

3.1. Yamazaki et al.'s (1996) experiments

Coarsening in a two-phase system consisting of the two main lower mantle minerals, perovskite and periclase, at $P = 25\,GPa$ (lower mantle conditions) was studied in the unique experiments by Yamazaki et al. (1996). The authors found that the grain size varies as a power-law function of time

$$d \sim t^{1/n} \tag{3}$$

with an extremely large n, around 11. This suggests that the grain size in the lower mantle is nearly constant and is around 20–50 μm. In the following sections, we review the mechanisms of grain growth and discuss possible explanations for the high n in Yamazaki et al.'s (1996) experiments.

3.2. One-phase systems

The "classical" value of grain growth exponent for pure metals or ceramics is 2 (Beck et al., 1948; Burke, 1949; Burke and Turnbull, 1952). It can be obtained with the assumption that the driving force ΔF (energy difference across curved interfaces) is inversely proportional to the grain size: $\Delta F \propto d^{-1}$. Assuming that the grain boundary velocity $V \sim \dot{d}$ is proportional to ΔF, we obtain $d \sim t^{1/2}$.

Much larger grain growth exponents are often observed in both pure metals and alloys (Hu and Rath, 1970; Higgins, 1974). For pure materials, this is believed to be due to a nonlinear relationship between the grain boundary velocity and the driving force, $V \propto \Delta F^m$, where m is a constant (Hu and Rath, 1970). This gives a more general result $n = m + 1$. For example, in the case of aluminum, $m \approx 12$ at $T = 0.4T_m$, and approaches $m = 1$ as the temperature approaches melting temperature.

Impurities is another factor which can increase n (Gordon, 1963). They tend to concentrate in the moving grain boundaries affecting the driving force and therefore the grain growth rate.

However, these factors cannot control the grain growth rate in the lower mantle—the observed interlocking and simultaneous growth of the perovskite

and magnesiowüstite grains imply that Ostwald ripening of the two phases and not the grain boundary migration is the rate controlling process. So, we have to consider grain growth in two-phase systems.

3.3. Two-phase systems

Before we discuss two-phase systems, we would like to note that the term "grain growth" is traditionally used for one-phase systems, where grains grow via grain boundary migration. Growth of second-phase particles is usually referred as "coarsening" or "Ostwald ripening". Sometimes, especially when both grain growth and coarsening take place at the same time, the terms "grain growth" and "coarsening" are used in a broader sense.

The coarsening exponent for Ostwald ripening of particles in polycrystalline matrix is $n = 3$ in case of volume diffusion controlled growth (Lifshitz and Slyozov, 1961; Wagner, 1961), $n = 4$ if the grain growth is controlled by grain boundary diffusion (Ardell, 1972) and $n = 5$ for diffusion on dislocations (Ardell, 1972).

Solomatov and Stevenson (1994) suggested that if growth is controlled by surface nucleation, then Ostwald ripening obeys a logarithmic rather than power-law function of time. In this case, the apparent value of n can be arbitrary large. The factor which could be responsible for this behavior is the complexity of the perovskite molecule: attaching individual atoms to the growing grain might be statistically less probable than assembling first a group of atoms and then attaching the group to the growing grain. A high fluidity of grain boundaries could facilitate this process. However, we are not aware of any evidence that this growth mechanism can operate at low supersaturation, typically for Ostwald ripening.

Grain growth in the major phase often occurs simultaneously with Ostwald ripening. The coupling between the two processes can be described as follows. If the second-phase particles were stable, grain growth in the major phase would stop as soon as the grain size reaches some maximum value which is proportional to the size of the particles (Zener pinning, see Smith, 1948). If the second-phase particles undergo Ostwald ripening, the grains of the major phase can grow as well. Hillert (1965) and Gladman (1966) proposed that after a sufficiently long time, grain growth in two-phase systems in which both phases grow simultaneously is controlled by Ostwald ripening of the dispersed particles and is coupled through Zener pinning. There is evidence for such coupled growth in laboratory experiments (Mader and Hornbogen, 1974; Holm et al., 1977; Grewal and Ankem, 1989, 1990a, 1990b; Higgins et al., 1992; Ankem, 1992; Alexander et al., 1994) and in numerical simulations based on the diffuse interface field method (Fan et al., 1998). The grain growth exponents for both phases are the same and correspond to one of the three mechanisms of Ostwald ripening described above.

3.4. Effect of elastic stress

A common explanation for extremely slow coarsening of microstructures is the elastic stress (Humphreys and Hatherly, 1996; Martin et al., 1997). Although the effect of elastic stress on grain growth in the Earth's mantle was described by various authors (Morris, 1992, 1995; Liu et al., 1998), they considered grain growth during a phase transformation. Grain growth can be affected by elastic stresses even after the phase transformation (Ardell et al., 1966). Elastic stresses suppress coarsening. This can be seen from the fact that the elastic energy of two particles is minimized when they have the same size. Therefore, large elastic misfits work against Ostwald ripening as has been observed in many experiments. For example, in Warlimont and Thomas's (1970) experiments, particles of an Fe_3Al phase in an Fe–Al system did not show any detectable coarsening even after long annealing times. In Martin and Humphreys' (1974) experiments on coarsening of Co in a Cu–Co system, Ostwald ripening ceased after the particles reached some critical size. Langdon's (1980) experiments on grain growth in a Zn-22% Al alloy are particularly interesting because of similarities with Yamazaki et al.'s (1996) experiments. Both systems were eutectoid, the fraction of the second phase was relatively large, the grains were very small, they seemed to interlock, and the coarsening exponent was extremely large, $n \approx 25$ for the Zn-22% Al alloy and $n \approx 11$ for perovskite–magnesiowüstite. Grain growth in Langdon's (1980) experiments occurred during deformation and was clearly affected by stress. Also, Langdon (1980) observed superplasticity which, although not studied by Yamazaki et al. (1996), can

also occur in the perovskite–magnesiowüstite system (Karato et al., 1995; Ito and Sato, 1991).

Numerical experiments support these conclusions. In particular, they show that elastic interactions between the grains can increase the time exponent n to very large values (say, 10 and higher) and can cause particle splitting which occurs to minimize elastic energy of the system (Miyazaki and Doi, 1989; Nishimori and Onuki, 1990, 1991). Elastic stress can even cause inverse coarsening, wherein small particles can grow at the expense of large particles (Wang et al., 1992; Su and Voorhees, 1996). It is also worth noting that the elastic energy of a two-phase system depends on its configuration. Microstructures generated by eutectoid decomposition are very coherent and generate elastically interlocked grains.

In the case of the perovskite–magnesiowüstite system studied by Yamazaki et al. (1996), the elastic stress can be introduced by the eutectoid decomposition of spinel to perovskite and magnesiowüstite. Spinel, perovskite and magnesiowüstite are all anisotropic minerals and have different properties including density and elastic constants. Additional stress could be introduced due to compression of the samples in the graphite capsule, however, the differential stress is tiny ($<$10 MPa, see Rubie et al., 1993) compared to the stresses due to volume misfit between the phases ($\sim$1 GPa).

The controlling parameter is the ratio of the elastic energy to the surface energy:

$$L = \frac{\epsilon^2 K d}{\sigma} \tag{4}$$

where ϵ is the strain, K an elastic constant, d the grain size and σ is the interfacial energy (Su and Voorhees, 1996). Large values of L indicate that the elastic stresses affect the grain growth. For example, for a simple two-dimensional system of only one, two or three particles, the critical value of L (for a particle shape bifurcation or inverse coarsening) is around 6.

Assuming $K \sim 10^{11}$ Pa, $d \sim 10^{-7}$ to 10^{-6} m, $\sigma \sim 1\,\mathrm{J\,m^{-2}}$, $\epsilon \sim 10^{-2}$ (the misfit between the phases), we obtain

$$L \sim 1\text{–}10 \tag{5}$$

which indicates that grain growth in Yamazaki et al.'s (2000) experiments could have been affected by elastic stresses.

A major difficulty with this explanation is viscous relaxation. At such a small grain size the viscosity is only about (Poirier, 1985):

$$\eta = 0.05\frac{d^2 k_\mathrm{B} T}{DV} \sim 10^{12}\text{–}10^{14}\ \mathrm{Pa\,s} \tag{6}$$

where $D \sim 10^{-18}\,\mathrm{m^3\,s^{-1}}$ (Yamazaki et al., 2000), $V \sim a^3$ is the atomic volume, $a \sim 2 \times 10^{-10}$ m is the interatomic distance (Anderson, 1989) and R is the gas constant. The Maxwell relaxation time, η/K, turns out to be quite small, in the order of 10–10^3 s. This is only marginally comparable with the duration of the experiments (10^2–10^5 s). Coble creep might reduce the relaxation time further by about 1 order of magnitude (provided diffusion along the grain boundaries is 4 orders of magnitude faster than volume diffusion, Yamazaki et al., 2000). This implies that the effect of the elastic stresses was probably small but given the uncertainties in the parameters cannot be excluded.

3.5. Effect of initial conditions

An unusually large apparent value of n could also be due to initial conditions and insufficient coarsening time. For example, a narrow initial particle size distribution can substantially slow down the coarsening rates in the early stages of Ostwald ripening (Fang and Patterson, 1993). Evolution of eutectoid structures is an even more complicated process. They undergo various morphological changes before nearly equiaxial grains develop and conventional Ostwald ripening is established (Graham and Kraft, 1966; Weatherly, 1975; Chattopadhyay and Sellars, 1982; Bartholomeusz and Wert, 1994; Whiting and Tsakiropoulos, 1997; Sharma et al., 2000). Further complications are due to the fact that crystallographic orientations of lamellar are usually not random but such as to minimize the surface energy (Weatherly, 1975; Martin et al., 1997). This contributes significantly to the stability of eutectoid structures and can also affect Ostwald ripening after degeneration of lamellae. It is unclear if the asymptotic regime of conventional Ostwald ripening has ever been reached in any laboratory experiments on coarsening of eutectoid structures and it is unclear if it happened in Yamazaki et al.'s (1996) experiments. An indirect

indication that lamellar structures generated by an eutectoid phase transformation is rather a special type of initial conditions (including geometry, elastic stress, and crystallographic orientations) is that coarsening in an analogue aggregate, $CaTiO_3$–FeO, which was produced mechanically showed "normal" values of n, from 2.2 to 3.5 (Wang et al., 1999).

4. Numerical simulations

4.1. The model

The numerical simulations described below provide an independent support for the Hillert (1965) and Gladman's (1966) proposal that asymptotic grain growth in two-phase systems is coupled through Zener pinning and is controlled by Ostwald ripening of the second-phase particles. The approach is based on Monte Carlo Potts model (Appendix A). The choice of parameters ensures that the critical grain size for the transition from the grain boundary diffusion regime to the volume diffusion regime is much higher than the typical grain size in the simulations. Therefore, at any time, Ostwald ripening is controlled by grain boundary diffusion. This simplifies the interpretation of the results by eliminating the transition from grain boundary diffusion regime to volume diffusion regime as a possible cause for the discrepancies between the numerical results and the asymptotic theory.

The structure of a two-dimensional two-phase system is represented with the help of a 400×400 square lattice. Each of the 160,000 lattice sites represents a group of atoms with a particular orientation (spin). When several adjacent sites have the same spin, they are considered a single grain. Although in reality, the range of spins is continuous, the results do not depend on the number of spins, Q, provided Q exceeds a value of about 50 (Anderson et al., 1984; Sahni et al., 1983; Grest et al., 1988). We found that a similar criterion is valid for two-phase systems. The value $Q = 100$ was used in all our simulations.

The physical properties of the phases can be quite different (for example, different species can be the bottle neck in the diffusion processes controlling the coarsening rates of the two phases). The interfacial energies are also known to depend on the misorientation angle. Since the physical properties of the perovskite/magnesiowüstite system are poorly constrained (see the discussion later), the controlling parameters of the two phases are chosen to be identical and all grain boundaries are assumed to have the same interfacial energy. In particular, this means that the case with a volume fraction of x% of the second phase is equivalent to one with a volume fraction of $(100 - x)$% of the dominant phase and vice versa.

4.2. Simulations of grain growth in two-phase systems

Fig. 1 illustrates the microstructural evolution of two-phase systems when the volume fraction of the second phase is between 5 and 50%. Fig. 2 gives the variation of the grain size with time. The standard deviation obtained after running each case three times is relatively small and is not shown. As can be seen from Fig. 2, in the beginning of evolution, the system passes through a transitional regime which is due to initial conditions and grain boundary migration in one-phase regions. The regime which is independent of the initial conditions and applicable to the Earth's mantle is the asymptotic regime.

To estimate the asymptotic grain growth exponent, we plotted the slope as a function of time (Fig. 3). The slope was calculated in a time window which was moving along the time axis. The logarithmic width, t_2/t_1, of the time window was about 2 in the beginning of evolution and 7 in the end of evolution when fluctuations are large (after $t \approx 10^3$–10^4 depending on the case). These calculations show that the asymptotic slope is close to the theoretical value 1/4 expected for grain-boundary diffusion controlled growth of particles embedded in a stable matrix. The cases with the lowest fractions of the second phase do not seem to fully reach the asymptotic regime (Fig. 3). For the one-phase system, the value of grain growth exponent ($\sim$0.5) agrees with previous numerical results for two-dimensional systems (Anderson et al., 1984; Sahni et al., 1983; Grest et al., 1988).

4.3. Is grain growth controlled by Zener pinning?

In this section, we compare the ratio of the grain size of the dominant phase to the grain size of the second phase with the one expected from Zener pinning.

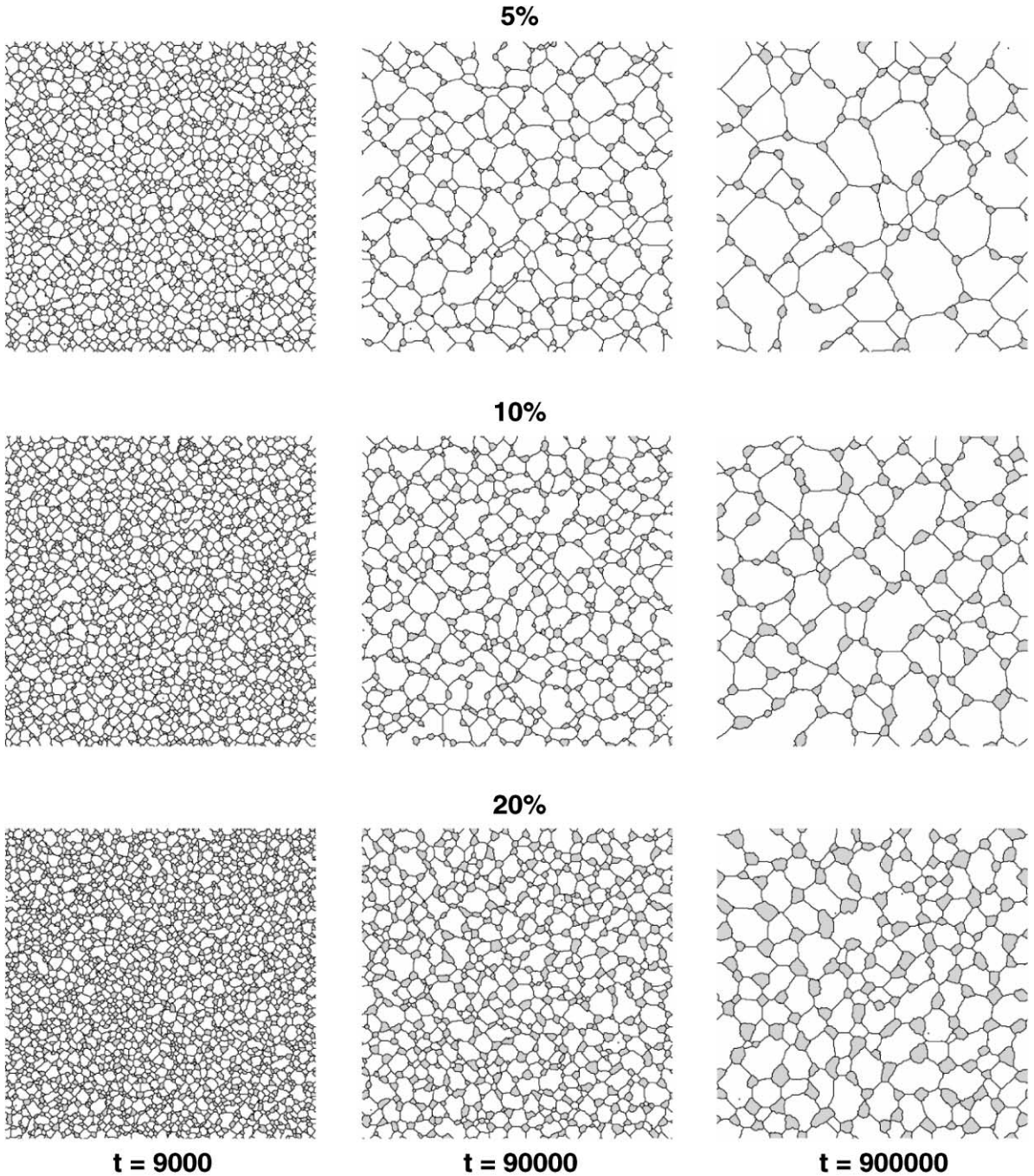

Fig. 1. Microstructural evolution of a system consisting of two phases, A (white) and B (grey), with various fractions of the second phase. Each row corresponds to one run. The boundary conditions are periodic in both vertical and horizontal directions (the square box used in our numerical simulations can be thought as a part of an infinite array of identical square boxes).

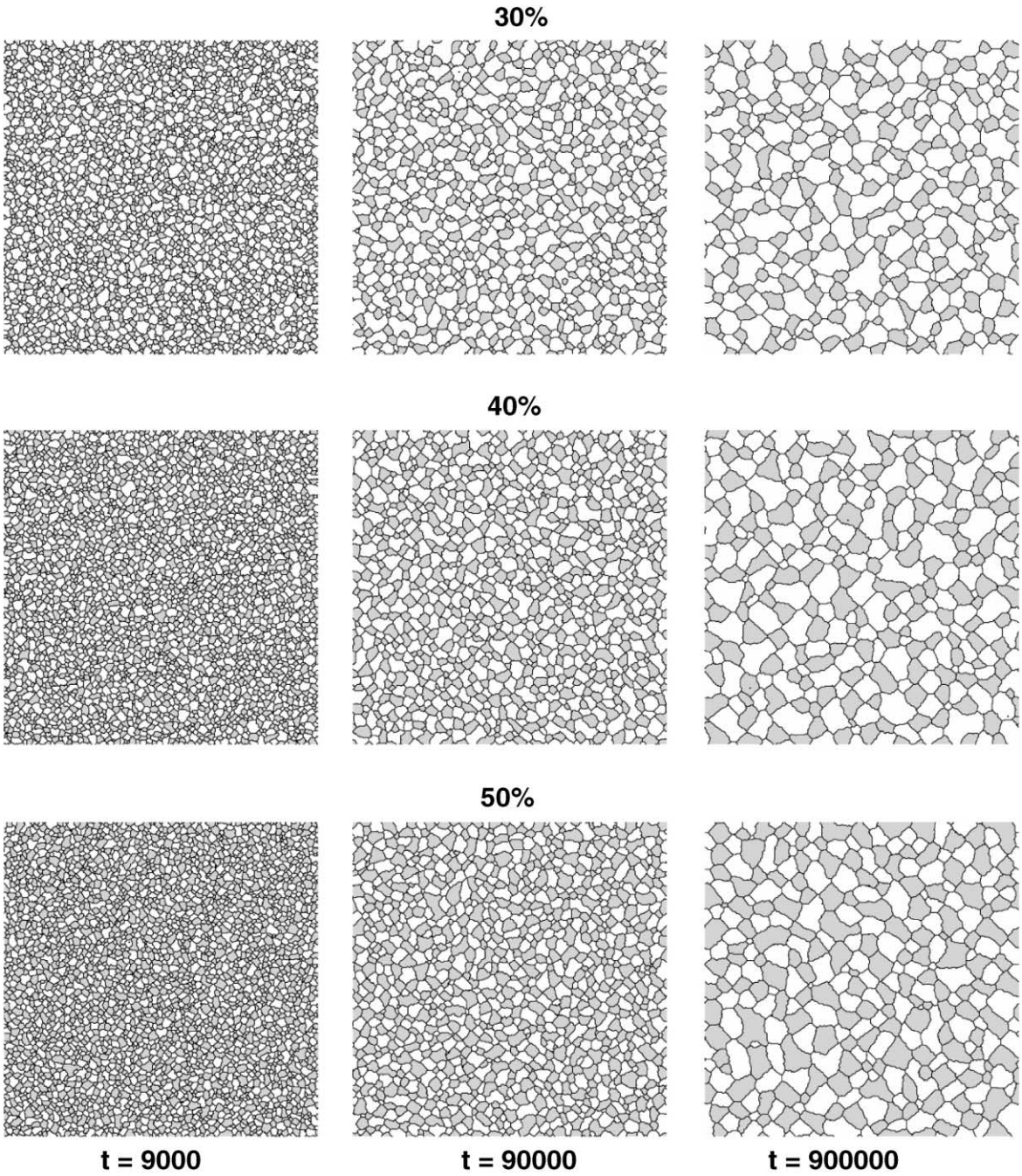

Fig. 1. (*Continued*).

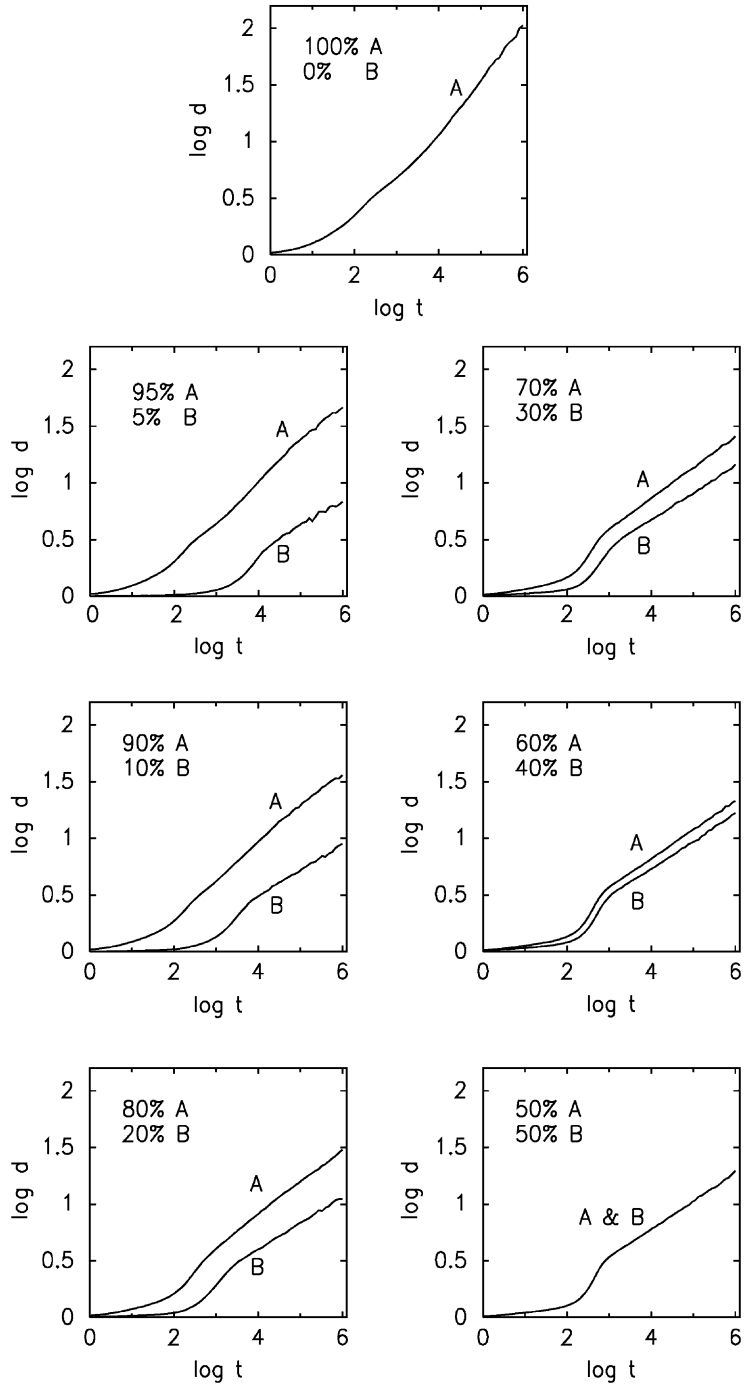

Fig. 2. The mean grain size as a function of time. The volume fraction of the phases are indicated.

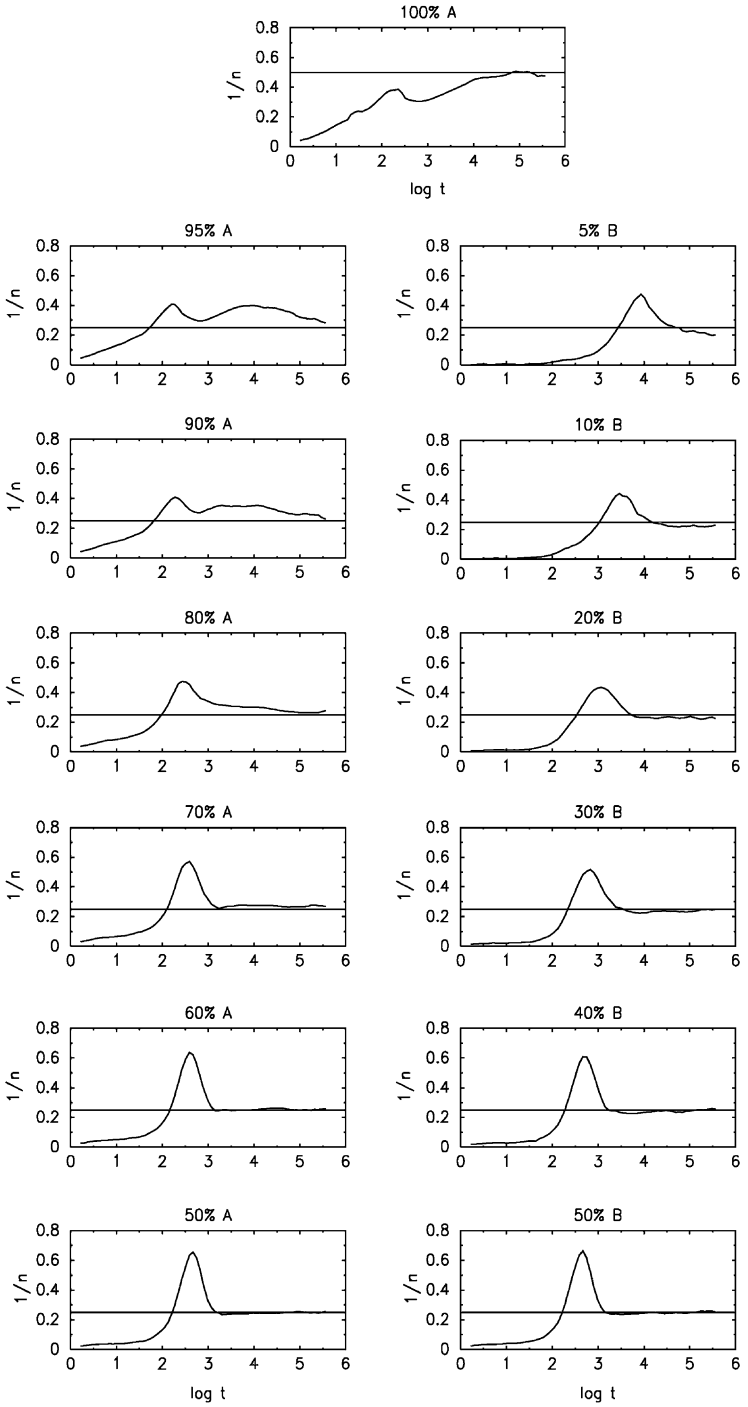

Fig. 3. The slope of the curves in Fig. 1 as a function of time for different volume fractions of the B phase. The horizontal solid lines show the theoretical value $1/n = 0.25$ for two-phase systems and $1/n = 0.5$ for the one-phase system.

If the second phase particles were stable (negligible growth), then the grains of the dominant phase would reach some maximum size and grain growth stops. This maximum size depends on various factors such as the shape and the distribution of the second-phase particles and is often described as

$$\frac{d_A}{d_B} = \frac{c}{\phi^\alpha} \tag{7}$$

where c is a numerical coefficient, α a constant whose value varies between 1/3 and 1, index A indicates the dominant phase and index B indicates the minor phase.

To estimate the ratio d_A/d_B for each of our cases, we picked a microstructure reached by a particular time and, using this microstructure as an initial condition, continued the run with fixed inter-phase boundaries. These fixed inter-phase boundaries simulate "stable second-phase particles". This procedure generates particle shape and distribution which are statistically similar to those which are established during Ostwald ripening.

After a small increase in the grain size due to grain boundary migration, the grain sizes of the phases become stable. The ratio d_A/d_B varied slightly from one run to another because of the variations in the distribution and the shape of particles established by grain growth. We did not find any significant dependence on the grain size (in agreement with theory). Evolution of the ratio d_A/d_B calculated from Fig. 3 and the range of d_A/d_B found from "stable second-phase particles" simulations are shown in Fig. 4. We conclude that the grain size of phase A indeed reaches and stabilizes near the maximum grain size established by Zener pinning. A very slow growth of d_A/d_B with time might be due to the fact the asymptotic regime of coupled Ostwald ripening has not been completely established.

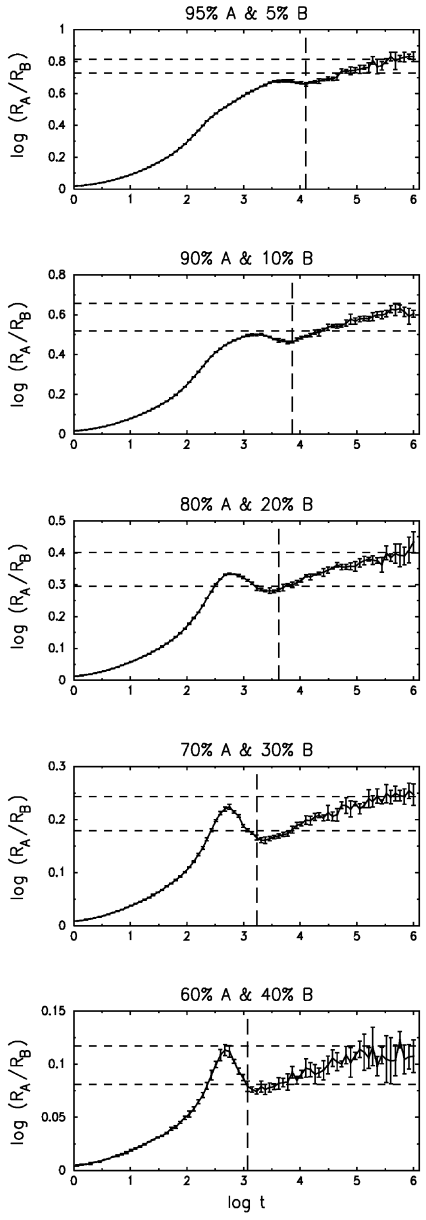

Fig. 4. Ratio of the grain size of phase A (d_A) to the grain size of phase B (d_B) versus time. The dashed lines indicate the range of grain size ratios obtained in simulations with "stable second-phase particles" (Zener pinning).

5. Grain growth in the lower mantle

5.1. The governing equations and physical parameters

In agreement with other previous studies, our results suggest that at sufficiently large times, grain growth of the dominant phase is coupled with grain growth of the minor phase via Zener pinning. Although we only studied grain boundary diffusion regime, the agreement with the theory suggests that the volume diffusion regime should give similar results but with the grain growth exponent 1/3 instead of 1/4. Therfore,

unless a surface nucleation mechanism is responsible for the slow grain growth in Yamazaki et al.'s (1996) experiments, the coarsening of perovskite is likely to obey a 1/4 or 1/3 law depending on whether Ostwald ripening is controlled by grain boundary diffusion or volume diffusion. The 1/5 law is a rather special case. In particular, it requires very high dislocation densities which are not expected in the lower mantle (the shear stresses are too small).

Ostwald ripening controlled by volume diffusion is described as (Lifshitz and Slyozov, 1961; Wagner, 1961; Voorhees, 1992)

$$d^3 - d_0^3 = \tfrac{32}{9} b_{\mathrm{V}}(\phi)\alpha D t \tag{8}$$

where

$$\alpha = \frac{2\sigma v_{\mathrm{m}} c_{\mathrm{e}}}{RT}, \tag{9}$$

v_{m} is the molar volume of the solute, c_{e} the equilibrium concentration of solute in the matrix, R the gas constant, $b_{\mathrm{V}}(\phi)$ a correction for a finite fraction of the second phase (Voorhees, 1992), such that $b_{\mathrm{V}}(0) = 1$, and d_0 is the initial diameter of the particles.

Ostwald ripening controlled by diffusion along grain boundaries is described as (Ardell, 1972)

$$d^4 - d_0^4 = \frac{64}{3\zeta} b_{\mathrm{GB}}(\phi)\alpha\delta D_{\mathrm{GB}} t \tag{10}$$

where $b_{\mathrm{GB}}(\phi)$ is a correction for a finite fraction of the second phase, D_{GB} the diffusion coefficient for diffusion along grain boundaries, ζ a geometrical factor of the order of unity, and δ is the width of the grain boundaries.

Since the lower mantle has two minor phases, magnesiowüstite and Ca-perovskite, the situation is more complicated. If we assume that there is little interaction between the two-phase domains formed by transformations in the grains of olivine and pyroxene subsystems (see Section 1), then grain growth of (Mg, Fe)-perovskite in each of these domains will be controlled by only one minor phase (magnesiowüstite or Ca-perovskite), the volume fraction of which is effectively 20–30%. However, if the interaction is important (which can happen when (Mg, Fe)-perovskite grains become comparable with the size of the original domains), then the grain size of (Mg, Fe)-perovskite will be controlled by both minor phases. In this case, the grain size of (Mg, Fe)-perovskite will mainly be controlled by the slowest growing phase.

The results of our simulations (Fig. 4) and previous experimental and theoretical estimates for Zener pinning (Olgaard and Evans, 1986) suggest that for typical volume fractions of magnesiowüstite and Ca-perovskite the grain size of (Mg, Fe)-perovskite is larger than the grain size of the second phase particles by a factor of 2–4. In Yamazaki et al.'s (1996) experiments, this ratio was between 1.2 and 1.5.

For the lower mantle, we assume the following values of the parameters: $\sigma \approx 1\,\mathrm{J\,m^{-2}}$, $v_{\mathrm{m}} \approx 2 \times 10^{-5}\,\mathrm{m^3\,mol^{-1}}$, $T \approx 2000\,\mathrm{K}$, $b_{\mathrm{V}} \approx 2$ and $t \approx 10^{15}\,\mathrm{s}$.

5.2. Uncertainties due to the presence of minor elements

At first glance, it seems that we only need to consider the major elements such as Si, O, Mg, Fe and Ca. Their solubilities in Mg-perovskite are in the order of 10^{-2} to 1 with Ca being the least soluble (e.g. Wood, 2000). However, in multicomponent systems, the effective values of c_{e} and D are quite complex functions of concentrations, diffusivities and the partition coefficients of the elements between the phases (Bartholomeusz and Wert, 1994; Lee et al., 1991). The basic reason why even minor elements can be the rate-controlling factor in Ostwald ripening is that the energy differences driving Ostwald ripening are very small.

A quantitative analysis of this problem for coarsening of Fe_3C (the precipitate) in steel (the matrix) in the presence of a third element M shows that the effective product $(c_{\mathrm{e}}D)_{\mathrm{M}}$ is determined by the following expression:

$$(c_{\mathrm{e}}D)_{\mathrm{M}} = \frac{D_{\mathrm{M}}^{\alpha}}{3(1-k)^2 u_{\mathrm{M}}^{\alpha}} \tag{11}$$

where D_{M}^{α} is the diffusion coefficient of the element M in the matrix, $k = u_{\mathrm{M}}^{\beta} u_{\mathrm{Fe}}^{\alpha} / u_{\mathrm{M}}^{\alpha} u_{\mathrm{Fe}}^{\beta}$ is the partition coefficient of the element M between the precipitate Fe_3C and the matrix, $u_{\mathrm{M}} = x_{\mathrm{M}}/(1 - x_{\mathrm{C}})$ and $u_{\mathrm{Fe}} = x_{\mathrm{Fe}}/(1 - x_{\mathrm{C}})$ are modified concentration parameters, and x_{M} and x_{C} are the mole fractions of M and C, respectively (Bartholomeusz and Wert, 1994). The superscript α indicates the matrix and β indicates the precipitate. A modified model which considers an arbitrary number of elements gives essentially similar results (Lee et al., 1991).

The implication for the lower mantle is that the minor and trace elements with the highest abundances and the lowest diffusivities and which partition mainly to magnesiowüstite and Ca-perovskite ($k \gg 1$) can control Ostwald ripening in the lower mantle.

5.3. The simplest model: Si is the rate-limiting species

If the low diffusivity of Si is more important than other factors, then we can estimate the grain size using the data from recent experiments by Yamazaki et al. (2000). For temperatures of 2000–2200 K and pressures corresponding to the top of the lower mantle, $D \sim 10^{-18}\,\mathrm{m^2\,s^{-1}}$ (Yamazaki et al., 2000). The fraction of Si in Mg- and Ca-perovskite is about 1/5 and it is presented in substantial (for Ostwald ripening) amounts in magnesiowüstite as well (in the order of 0.02, Wood, 2000). This gives the size of the second phase particles of about 80–160 μm. The size of the perovskite grains is then in the order of 10^2–10^3 μm.

For grain boundary diffusion to dominate over volume diffusion, the grain size must be smaller than $\delta D_{\mathrm{GB}}/D \sim 3\,\mu\mathrm{m}$, where $\delta \sim 3 \times 10^{-10}\,\mathrm{m}$ is the width of the grain boundaries and $D_{\mathrm{GB}}/D \sim 10^4\,\mu\mathrm{m}$ (Yamazaki et al., 2000). This critical grain size, $\sim$3 μm, is about 2 orders of magnitude smaller than the grain size estimated above. Therefore, if diffusion of silicon is the rate-limiting process, grain growth in perovskite is unlikely to be significantly affected by grain boundary diffusion.

However, the uncertainties are large. Any additional factor in the chain of kinetic processes such as diffusion of other species or interface reactions would tend to reduce the growth rates. On the other hand, particle migration and coalescence (Higgins et al., 1992) as well as superplastic creep (Caceras and Wilkinson, 1984) can accelerate grain growth.

Fig. 5 shows the grain size in the lower mantle as a function of $c_{\mathrm{e}}D$ and the initial grain size. All physical parameters are assumed to be constant. The starting point is the phase transformation at 660 km depth which determines the initial grain size of minor phases. The grains are supposed to make an 8000 km trip in the lower mantle before they return to the upper mantle. Although the calculations are very idealistic, they clearly illustrate the interplay between the initial grain size and the diffusion rates.

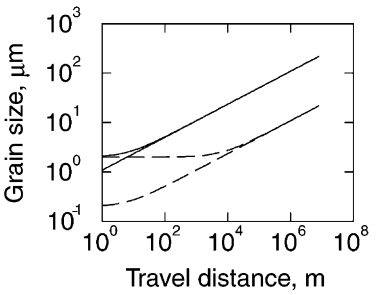

Fig. 5. An example of calculations of the grain size of perovskite as a function of the travel distance in the lower mantle. Ostwald ripening of magnesiowüstite is assumed to be the rate-controlling process. The initial grain size of magnesiowüstite after spheroidization of the eutectoid structure is 0.1 and 1 μm. The corresponding initial grain size of perovskite is 0.2 and 2 μm. The effective product $c_{\mathrm{e}}D$ for the rate-controlling species is 10^{-20} (solid curve) and 10^{-23} (dashed curve). The convective velocity is 5 cm per year. Other parameters are the same as in text.

5.4. Can elastic stress affect grain growth in the lower mantle?

Although the Maxwell relaxation time for the lower mantle is only 10^3–10^4 years, a shear stress is always present due to convection. If we assume that the negative buoyancy of the subducting slabs is mainly due to temperature and that it is in approximate balance with viscous stress then the viscous stress scales as

$$\tau \approx a\alpha\,\Delta T \rho g l \sim 3\,\mathrm{MPa}$$

where $\Delta T \approx 1400\,\mathrm{K}$ is the temperature contrast between the mantle and the Earth's surface, $\alpha \approx 2\times10^{-5}\,\mathrm{K^{-1}}$ the coefficient of thermal expansion, $g \approx 10\,\mathrm{m\,s^{-2}}$ the acceleration due to gravity, $l \approx 10^5\,\mathrm{m}$ the thickness of the subducting slabs and the numerical coefficient a is about 0.03 (estimated for small viscosity contrast regime of temperature-dependent viscosity convection, Moresi and Solomatov, 1995).

The ratio of the elastic energy to the interfacial energy is about $\tau^2 d/K\sigma \sim 10^{-2}$ to 10^{-1} for $d \sim 10^{-4}$ to 10^{-3} m. This implies that the effect of elastic stress is probably small on average but could be important in those regions of the lower mantle where the grain size reaches 10^{-2} m (which is not unusual for the upper mantle; Karato, 1984, 1989; Karato and Wu, 1993) or where the stresses are high (for instance, in the subducting plates as evident from the magnitudes of stress drop during earthquakes; Kanamori, 1994).

6. Conclusion

Numerical experiments in two-phase aggregates confirmed a previously suggested idea that the coarsening rate of the dominant phase is determined by Zener pinning and Ostwald ripening of the second phase particles. This implies that the grain size of (Mg, Fe)-perovskite is determined by Ostwald ripening of magnesiowüstite and Ca-perovskite.

The physical parameters controlling Ostwald ripening are poorly constrained. If silicon is the slowest diffusion species then grain growth is likely to follow $d \propto t^{1/3}$ law and the grain size of (Mg, Fe)-perovskite grains is likely to be 100–1000 μm.

Constraining the grain size in the lower mantle appears to be a very challenging problem. One major difficulty is that application of the laboratory results to the mantle is subject to large errors when extrapolated from small time scales of laboratory experiments to large time scales of the convective mantle. For example, the elastic stress due to volume misfit between the phases, the special geometry consisting of lamellae of alternating perovskite and magnesiowüstite and special crystallographic orientations of lamellae can have a large effect on the initial grain growth immediately after the spinel–perovskite phase transformation but would eventually disappear on large time scales. Any of these factors can be responsible for a very high value of grain growth exponent $n \sim 11$ in the only experiments on perovskite–magnesiowüstite system (Yamazaki et al., 1996). It is also difficult to identify the rate-controlling process in multicomponent systems. Tiny energy differences associated with grain growth imply that diffusion of not only a major element but also some minor element can be the rate-controlling process.

What can be done to improve the constraints on the grain size in the lower mantle? Despite the limitations of the direct experiments on grain growth in the lower mantle materials, these experiments provide the most valuable data. The time scale problem can be overcome with the help of numerical models which can investigate grain growth beyond the small time scales of laboratory experiments. Future numerical models need to include the effects which are present on small time scales but disappear on large time scales (lamellar structure, elastic stress, etc.). This would help to build a bridge between the laboratory and mantle time scales and would help to fully use the information provided by the laboratory experiments. It is also important to extend the simulations to three dimensions. Although grain growth exponents are unlikely to change, some processes such as Zener pinning, are not accurately described by two-dimensional models (Tikare et al., 2001). Constraints on the rate-controlling processes can be obtained by measuring the diffusivities and partition coefficients of those elements which are the likely candidates for the rate-controlling species (e.g. Yamazaki et al., 2000).

7. Further reading

Björklund, S., Donaghey, L.F., Hillert, M., 1972. The effect of alloying elements on the rate of Ostwald ripening of cementite in steel. Acta Metall. 20, 867–874.

Acknowledgements

The authors thank U.H. Faul and S.-I. Karato for thoughtful and constructive reviews. This work was supported by the NASA Grant NAG5-8803, Alfred P. Sloan Foundation, NERC (UK) and Sandia National Laboratories.

Appendix A. Numerical model

The numerical method used in this study is based on the Monte Carlo approach which has been successful for this type of problem (Anderson et al., 1984, 1989; Tikare and Cawley, 1998a, 1998b; Tikare et al., 1998). This method is also known as the large-Q Potts model. The model described below is essentially similar to one developed by Tikare and Cawley (1998b) for grain growth in solids in the presence of a liquid phase. The only difference is that in our model the second phase is not liquid but solid. In particular, it has grain boundaries which would be absent in the liquid phase.

The two-phase aggregate is treated as a two-dimensional square array of sites. A site represents a domain with a particular orientation of crystalline lattice. Ideally, a site should correspond to an atom. However, the statistics of migration of a group of atoms is sim-

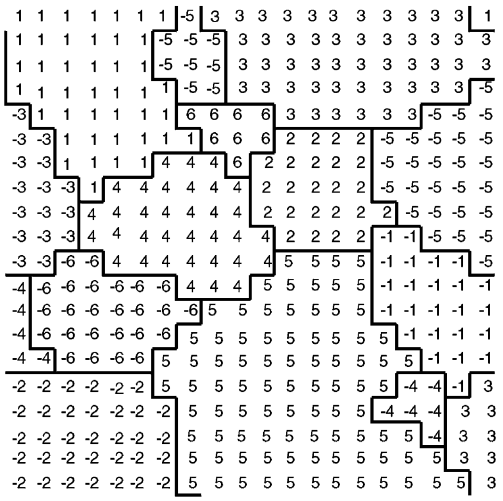

Fig. 6. Monte Carlo Potts model with a square lattice. A cluster of sites with the same index (spin) represents one grain. Positive spins indicate phase A. Negative spins indicate phase B.

ilar to the statistics of migration of individual atoms. The orientation of the individual grains is described with the help of "spin". Each site is given a random number (spin), between 1 and Q, as shown in Fig. 6. A grain can consist of one or more sites with the same spin. A grain boundary is therefore a boundary which separates regions with different spins. The sites representing the major phase (phase A) are assigned positive spins. The sites representing the second phase (phase B) are assigned negative numbers.

The total interfacial energy of the system can be expressed as follows:

$$E_{\text{total}} = \frac{1}{2}\sum_{i=1}^{N}\sum_{j=1}^{z} E(i,j)[1-\delta(q_i - q_j)] \qquad \text{(A.1)}$$

where $E(i, j)$ is the boundary energy between sites i and j, q_i the spin of the ith site, N the total number of lattice sites, z the number of nearest neighbors and δ is the Kronecker delta function.

Four orthogonal and four diagonal neighbors are considered in the calculation of the total energy so that the number of nearest neighbors, z, equals 8. We consider the simplest case in which all boundaries have the same energy, $E(i, j) = E_0$.

The microstructural evolution occurs as a result of two processes: grain boundary migration and long-range diffusion. Grain boundary migration occurs as a result of spin flip within one phase. Consider, for example, the boundary between the grains with spin $s = 4$ and 5 in the center of Fig. 6. This boundary would propagate upward if one of the sites with $s = 4$ would change its spin to $s = 5$. Numerically this is done by randomly selecting a site and flipping it to a different randomly chosen spin. The new spin is chosen from all possible spins, from 1 to Q (or from -1 to $-Q$). The spin is not allowed to change its sign—that would mean growth of one phase for the expense of the other. The change ΔE_{total} in interfacial energy is then calculated using Eq. (A.1). The probability for the spin flip is calculated with the help of a step-like function which only allows flips at the boundaries

$$P(\Delta E) = \begin{cases} 1, & \Delta E \le 0 \\ 0, & \Delta E > 0 \end{cases} \qquad \text{(A.2)}$$

The second process is long-range diffusion which transports material from one grain to another through the grains of the other phase. This requires spin exchange between the phases. Numerically this is done as follows. A site and its neighbor are selected at random. If they belong to different phases, they are allowed to exchange their spins. This can create an isolated spin of phase B. This spin can randomly walk through the matrix of phase A until it reaches another (or the same—depending on the result of random walking) grain of phase B. The probability function for spin exchange must have a non-zero probability for the events with positive energy difference. Otherwise there would be no exchanges. Therefore, instead of using the simplified probability function Eq. (A.2), it is necessary to use the full Arrhenius function determined by Boltzmann statistics

$$P(\Delta E) = \begin{cases} 1, & \Delta E \le 0 \\ \exp\left(\dfrac{-\Delta E}{k_{\text{B}}T}\right), & \Delta E > 0, \end{cases} \qquad \text{(A.3)}$$

where k_{B} is the Boltzmann constant and T is the temperature. If the energy change ΔE is negative or zero the move is accepted. If the energy change is positive, a random number x between 0 and 1 is drawn, and only the move for which $\exp(-\Delta E/k_{\text{B}}T) \ge x$ is accepted. Otherwise the move is rejected.

The unit of time in the simulation is the Monte Carlo Step (MCS) which represents N attempted transitions, where N is the number of lattice sites in the model.

Time is incremented after each attempted spin flip by $1/N$ MCS.

The temperature in Eq. (A.3) is chosen as follows. On the one hand, it must be high enough to avoid the low-temperature regime. In the low temperature regime, Monte Carlo models give very low-grain growth exponents (Tikare and Cawley, 1998b), perhaps, because of an insufficient amount of the dissolved material. On the other hand, if we want to delay the transition from the grain boundary diffusion regime to the volume diffusion regime the temperature should not be too high. (The time interval when the asymptotic regime of Ostwald ripening can take place is already small in our simulations. The presence of the second asymptotic regime in which volume diffusion dominates or the transition to this regime would make the results difficult to interpret.) The value $T = 0.7$ satisfies both requirements.

References

Alexander, K.B., Becher, P.F., Waters, S.B., Bleier, A., 1994. Grain growth kinetics in alumina–zirconia (CeZTA) composites. J. Am. Ceram. Soc. 77, 939–946.

Anderson, D.L., 1989. Theory of the Earth. Blackwell Scientific, Boston, MA.

Anderson, M.P., Srolovitz, D.J., Grest, G.S., Sahni, P.S., 1984. Computer simulation of grain growth. I. Kinetics. Acta Metall. 32 (5), 783–791.

Anderson, M.P., Grest, G.S., Srolovitz, D.J., 1989. Computer simulation of grain growth in three dimensions. Phil. Mag. 59B, 293–329.

Ankem, S., 1992. Grain growth in multiphase alloys. Mater. Sci. Forum 92–96, 159–168 .

Ardell, A.J., 1972. On the coarsening of grain boundary precipitates. Acta Metall. 20, 601–609.

Ardell, A.J., Nicholson, R.B., Eshelby, J.D., 1966. On the modified structure of aged Ni–Al alloys (with an appendix on the elastic interaction between inclusions). Acta Metall. 14, 1295–1309.

Bartholomeusz, M.F., Wert, J.A., 1994. The effect of thermal exposure on microstructural stability and creep resistance of a two-phase TiAl/Ti_3Al lamellar alloy. Metall. Mater. Trans. A 2371–2381.

Beck, P.A., Kremer, J.C., Demer, L.J., Holzworth, M.L., 1948. Grain growth in high-purity aluminum and in an aluminum–magnesium alloy. Trans. AIME 175, 372–394.

Braun, J., Chery, J., Poliakov, A., Mainprice, D., Vauchez, A., Tomassi, A., Daignieres, M., 1999. A simple parameterization of strain localization in the ductile regime due to grain size reduction a case study for olivine. J. Geophys. Res. 104, 25167–25181.

Burke, J.E., 1949. Some factors affecting the rate of grain growth in metals. Trans. Metall. Soc. AIME 180, 73–91.

Burke, J.E., Turnbull, D., 1952. Recrystallization and grain growth. Prog. Metal. Phys. 3, 220–292.

Caceras, C.H., Wilkinson, D.S., 1984. Large strain behavior of a superplastic alloy. 1. Deformation. Acta Metall. 32, 415–434.

Chattopadhyay, S., Sellars, C.M., 1982. Kinetics of pearlite spheroidization during static annealing and during hot deformation. Acta Metall. 30, 157–170.

Christensen, U.R., 1984. Heat transfer by variable viscosity convection and implication for the Earth's thermal evolution. Phys. Earth Planet. Inter. 35, 264–282.

Cooper, R.F., Kohlstedt, D.L., 1982. Interfacial energies in the olivine–basalt system. In: Akimoto, S., Manghnani, M.H. (Eds.), High Pressure Research in Geophysics. Center for Academic Publishing, Tokyo, pp. 217–228.

Daessler, R., Yuen, D.A., Karato, S., Riedel, M.R., 1996. Two-dimensional thermo-kinetic model for the olivine–spinel phase transition in subducting slabs. Phys. Earth Planet. Inter. 94, 217–239.

Derby, B., Ashby, M.F., 1987. On dynamic recrystallization. Scr. Metall. 21, 879–884.

Fan, D., Chen, L.Q., Chen, S.P.P., 1998. Numerical simulation of Zener pinning with growing second-phase particles. J. Am. Ceram. Soc. 81, 526–532.

Fang, Z.G., Patterson, B.R., 1993. Experimental investigation of particle-size distribution influence on diffusion-controlled coarsening. Acta Metall. 41, 2017–2024.

Gladman, T., 1966. On the theory of the effect of precipitate particles on grain growth in metals. Proc. R. Soc. London 294A, 298–309.

Gordon, P., 1963. A rationalization of the data on grain boundary migration in zone-refined metals as influenced by dissolved impurities. Trans. Met. Soc. AIME 227, 699–705.

Graham, L.D., Kraft, R.W., 1966. Coarsening of eutectic microstructures at elevated temperatures. Trans. Metall. Soc. AIME 236, 94–102.

Grest, G.S., Anderson, M.P., Srolovitz, D.J., 1988. Domain-growth kinetics for the Q-state Potts model in two and three dimensions. Phys. Rev. 38B, 4752–4760.

Grewal, G., Ankem, S., 1989. Isothermal particle growth in two-phase titanium alloys. Metall. Trans. 20A, 39–54.

Grewal, G., Ankem, S., 1990a. Particle coarsening behavior of α–β titanium alloys. Metall. Trans. 21A, 1645–1654.

Grewal, G., Ankem, S., 1990b. Modeling matrix grain growth in the presence of growing second phase particles in two-phase alloys. Acta Metall. 38, 1607–1617.

Higgins, G.T., 1974. Grain-boundary migration and grain growth. Metal Sci. 8, 143–150.

Higgins, G.T., Wiryolukito, S., Nash, P., 1992. The kinetics of coupled phase coarsening in two-phase structures. Mater. Sci. Forum 92–96, 671–676.

Hillert, M., 1965. On the theory of normal and abnormal grain growth. Acta Metall. 13, 227–238.

Hillert, M., 1972. On theories of growth during discontinuous precipitation. Metall. Trans. 3, 2729–2741.

Hogrefe, A., Rubie, D.C., Sharp, T.G., Seifert, F., 1994. Metastability of enstatite in deep subducting lithosphere. Nature 372, 351–353.

Holm, K., Embury, J.D., Purdy, G.R., 1977. The structure and properties of microduplex Zr–Nb alloys. Acta Metall. 25, 1191–1200.

Hu, H., Rath, B.B., 1970. On the time exponent in isothermal grain growth. Metall. Trans. 1, 3181–3184.

Humphreys, F.J., Hatherly, M., 1996. Recrystallization and Related Annealing Phenomena. Pergamon Press, New York.

Irifune, T., 1994. Absence of an aluminous phase in the upper part of the Earth's lower mantle. Nature 370, 131–133.

Irifune, T., Ringwood, T.A., 1987a. Phase transformations in a harzburgite composition to 26 GPa implications for dynamical behavior of the subducting slab. Earth Planet. Sci. Lett. 86, 365–376.

Irifune, T., Ringwood, T.A., 1987b. Phase transformations in primitive MORB and pyrolite compositions to 25 GPa and some geophysical implications. In: Manghnani, M.H., Syono, Y. (Eds.), High Pressure Research in Mineral Physics. Am. Geophys. Union, Geophys. Monogr. Ser. 39, pp. 231–242.

Ita, J., Stixrude, L., 1993. Density and elasticity of model upper mantle compositions and their implications for whole mantle structure. In: Evolution of the Earth and Planets. Am. Geophys. Union Geophys. Monogr. Ser. 74, pp. 111–130.

Ito, E., Sato, H., 1991. Aseismicity in the lower mantle by superplasticity of the descending slab. Nature 351, 140–141.

Ito, E., Takahashi, E., 1987. Ultrahighpressure phase transformations and the constitution of the deep mantle. In: Manghnani, M.H., Syono, Y. (Eds.), High Pressure Research in Mineral Physics. Am. Geophys. Union, Geophys. Monogr. Ser. 39, pp. 221–230.

Ito, E., Takahashi, E., 1989. Postspinel transformations in the system Mg_2SiO_4–Fe_2SiO_4 and some geophysical implications. J. Geophys. Res 94, 10637–10646.

Ito, E., Akaogi, M., Topor, L., Navrotsky, A., 1990. Negative pressuretemperature slopes for reactions forming $MgSiO_3$-perovskite from calorimetry. Science 249, 1275–1278.

Jackson, I., Rigden, S.M., 1998. Composition and temperature of the Earth's mantle seismological models interpreted through experimental studies of Earth materials. In: Jackson, I. (Ed.), The Earth's Mantle. Cambridge University Press, New York, pp. 405–460.

Kameyama, M., Yuen, D.A., Fujimoto, H., 1997. The interaction of viscous heating with grain-size dependent rheology in the formation of localized slip zones. Gephys. Res. Lett. 24, 2523–2526.

Kanamori, H., 1994. Mechanics of earthquakes. Annu. Rev. Earth Planet. Sci. 22, 207–237.

Karato, S.-I., 1984. Grain-size distribution and rheology of the upper mantle. Tectonophys. 104, 155–176.

Karato, S.-I., 1989. Grain growth kinetics in olivine aggregates. Tectonophys. 168, 255–273.

Karato, S.-I., 1997. Phase transformations and rheological properties of mantle materials. In: Crossley, D.J. (Ed.), Earth's Deep Interior, Gordon and Breach, London, pp. 223–272.

Karato, S.-I., Wu, P., 1993. Rheology of the upper mantle: a synthesis. Science 260, 771–778.

Karato, S., Zhang, S., Wenk, H.-R., 1995. Superplasticity in Earth's lower mantle evidence from seismic anisotropy and rock physics. Science 270, 458–461.

King, S.D., 1995. Models of mantle viscosity. In: Ahrens, T.J. (Ed.), Mineral Physics and Crystallography: A Handbook of Physical Constants, Vol. 2. Am. Geophys. Union. Ref. Shelf, pp. 227–236.

Kubo, A., Akaogi, M., 2000. Post-garnet transitions in the system $Mg_4Si_4O_{12}$–$Mg_3Al_2Si_3O_{12}$ up to 28 GPa phase relations of garnet, ilmenite and perovskite. Phys. Earth Planet. Inter. 121, 85–102.

Kubo, T., Ohtani, E., Kato, T., Urakawa, S., Suzuki, A., Kanbe, Y., Funakoshi, K.-I., Utsumi, W., Fujino, K., 2000. Formation of metastable assemblages and mechanisms of the grain-size reduction in the postspinel transformation of Mg_2SiO_4. Geophys. Res. Lett. 27, 807–810.

Langdon, T.G., 1980. The influence of grain growth on the mechanical properties of two-phase superplastic alloys. In: Hansen, N., Jones, A.R., Leffers, T. (Eds.), Recrystallization and Grain Growth of Multi-Phase and Particle Containing Materials. Proceedings of the 1st Riso International Symposium on Metallurgy and Materials Science. Riso National Laboratory, pp. 223–228.

Lee, H.M., Allen, S.M., Grujicic, M., 1991. Coarsening resistance of M_2C carbides in secondary hardening steels. Part I. Theoretical model for multicomponent coarsening kinetics. Metall. Trans. 22, 2863–2868.

Lifshitz, I.M., Slyozov, V.V., 1961. The kinetics of precipitation from supersaturated solid solution. J. Phys. Chem. Solids 19, 35–50.

Liu, M., Kerschhofer, L., Mosenfelder, J.L., Rubie, D.C., 1998. The effect of strain energy on growth rates during the olivine–spinel transformation and implications for olivine metastability in subducting slabs. J. Geophys. Res. 103, 23897–23909 .

Livingston, J.D., Cahn, J.W., 1974. Discontinuous coarsening of aligned eutectoids. Acta Metall. 22, 495–503.

Mader, K., Hornbogen, E., 1974. Systematics of recrystallization micromechanisms in $\alpha + \beta$ brass. Scripta Metall. 8, 979–984.

Manga, M., 1996. Mixing of heterogeneities in the mantle Effect of viscosity differences. Geophys. Res. Lett. 23, 403–406.

Martin, J.W., Humphreys, F.J., 1974. Stabilization of an array of equiaxed precipitates in the system Cu–Co. Scripta Metall. 8, 679–680.

Martin, J.W., Doherty, R.D., Cantor, B., 1997. Stability of Macrostructure in Metallic Systems. Cambridge University Press, New York.

Martinez, I., Wang, Y., Guyot, F., Liebermann, R.C., 1997. Microstructures and iron partitioning in (Mg, Fe)SiO_3-perovskite–(Mg, Fe)O-magnesiowüstite assemblages an analytical transmission electron microscopy study. J. Geophys. Res. 102, 5265–5280.

Meade, C., Silver, P.G., Kaneshima, S., 1995. Laboratory and seismological observations of lower mantle isotropy. Geophys. Res. Lett. 22, 1293–1296.

Miyazaki, T., Doi, M., 1989. Shape bifurcations in the coarsening of precipitates in elastically constrained systems. Mater. Sci. Eng. 110A, 175–185.

Moresi, L.-N., Solomatov, V.S., 1995. Numerical investigation of 2D convection with extremely large viscosity variations. Phys. Fluids 7, 2154–2162.

Morris, S., 1992. Stress relief during solid-state transformations in minerals. Proc. R. Soc. London 43A, 203–216.

Morris, S., 1995. The relaxation of a decompressed inclusion. Zeit. Ang. Math. Phys. 46, S335–S355.

Nieh, T.G., Wadsworth J., Sherby, O.D., 1997. Superplasticity in Metals and Ceramics. Cambridge University Press, New York.

Nishimori, H., Onuki, A., 1990. Pattern formation in phase-separating alloys with cubic symmetry. Phys. Rev. 42B, 980–983.

Nishimori, H., Onuki, A., 1991. Freezing of domain growth in cubic solids with elastic misfit. J. Phys. Soc. Japan 60, 1208–1211.

Olgaard, D., Evans, B., 1986. Effect of second-phase particles on grain growth in calcite. J. Am. Ceram. Soc. 691, C272–C277.

Poirier, J.P., 1985. Creep of Crystals. Cambridge Univeraity Press, Cambridge.

Poirier, J.P., Peyronneau, J., Madon, M., Guyot, F., Revcolevschi, A., 1986. Eutectoid phase transformation of olivine and spinel into perovskite and rock salt structure. Nature 321, 603–605.

Porter, D.A., Easterling, K.E., 1997. Phase Transformations in Metals and Alloys. Chapman and Hall, New York.

Puls, M.P., Kirkaldy, J.S., 1972. The pearlite reaction. Metall. Trans. 3, 2777–2796.

Riedel, M.R., Karato, S., 1997. Grain-size evolution in subducted oceanic lithosphere associated with the olivine–spinel transformation and its effects on rheology. Earth Planet. Sci. Lett. 148, 27–43 .

Rubie, D.C., 1993. Mechanisms of kinetics of reconstructive phase transformations in the Earth's mantle. In: Luth, R.W. (Ed.), Experiments at High Pressure and Applications to the Earth's mantle. Mineral Association of Canada Short Course Handbook, Vol. 21, pp. 247–303.

Rubie, D.C., Ross, C.R., 1994. Kinetics of the olivine–spinel transformation in subducting lithosphere experimental constraints and implications for deep slab processes. Phys. Earth Planet. Inter. 86, 223–241.

Rubie, D.C., Karato, S., Yan, H., O'Neill, H.S.C., 1993. Low differential stress and controlled chemical environment in multianvil high-pressure experiments. Phys. Chem. Miner. 20, 315–322.

Sahni, P.S., Srolovitz, J.D., Grest, G.S., Anderson, M.P., Safran, S.A., 1983. Kinetics of ordering in two dimensions. II. Quenched systems. Phys. Rev. 28B, 2705–2716.

Sharma, G., Ramanujan, R.V., Tiwari, G.P., 2000. Instability mechanisms in lamellar microstructures. Acta Mater. 48, 875–889.

Shimizu, I., 1998. Stress and temperature dependence of recrystallized grain size: a subgrain misorientation model. Geophys. Res. Lett. 25, 4237–4240.

Smith, C.S., 1948. Grains, phases and interfaces an interpretation of microstructures. Trans. AIME 175, 15–51.

Solomatov, V.S., 1996. Can hotter mantle have a larger viscosity? Geophys. Res. Lett. 23, 937–940.

Solomatov, V.S., 2001. Grain size-dependent viscosity convection and the thermal evolution of the Earth. Earth Planet. Sci. Lett. 191, 203–212.

Solomatov, V.S., Moresi, L.-N., 1997. Three regimes of mantle convection with non-Newtonian viscosity and stagnant lid convection on the terrestrial planets. Geophys. Res. Lett. 24, 1907–1910.

Solomatov, V.S., Stevenson, D.J., 1993. Kinetics of crystal growth in a terrestrial magma ocean. J. Geophys. Res. 98, 5407–5418.

Solomatov, V.S., Stevenson, D.J., 1994. Can sharp seismic discontinuities be caused by non-equilibrium phase transformations? Earth Planet. Sci. Lett. 125, 267–279.

Su, C.H., Voorhees, P.W., 1996. The dynamics of precipitate in elastically stressed solid. I. Inverse coarsening. Acta Mater. 44, 1987–1999.

Sundquist, B.E., 1968. The edgewise growth of pearlite. Acta Metall. 16, 1413–1427.

Tikare, V., Cawley, J.D., 1998a. Application of the Potts model to simulation of Ostwald ripening. J. Am. Ceram. Soc. 81, 485–491.

Tikare, V., Cawley, J.D., 1998b. Numerical simulations of grain growth in liquid phase sintered materials. II. Study if isotropic grain growth. Acta Mater. 46, 1343–1356.

Tikare, V., Holm, E.A., Fan, D., Chen, L.Q., 1998. Comparison of phase-field and Potts models for coarsening processes. Acta Mater. 47, 363–371.

Tikare, V., Miodownik, M.A., Holm, E.A., 2001. Three-dimensional simulation of grain growth in the presence of mobile pores. J. Am. Ceram. Soc. 84, 1379–1385.

Voorhees, P.W., 1992. Ostwald ripening of two-phase mixtures. Annu. Rev. Mater. Sci. 22, 197–215.

Wagner, C., 1961. Theorio der alterung von niederschlägen durch umlösen. Electrochem. 65, 581–591.

Wang, Y., Chen, L.-Q., Khachaturyan, A.G., 1992. Particle translational motion and reverse coarsening phenomena in multiparticle systems induced by a long-range elastic interaction. Phys. Rev. 17B, 11194–11197.

Wang, Y., Martinez, I., Guyot, F., Liebermann, R.C., 1997. The breakdown of olivine to perovskite and magnesiowüstite. Science 275, 510–513.

Wang, Z.-C., Mei, S., Karato, S., Wirth, R., 1999. Grain growth in $CaTiO_3$-perovskite + FeO-magnesiowüstite aggregates. Phys. Chem. Miner. 27, 11–19.

Warlimont, H., Thomas, G., 1970. Twophase microstructures of α-FeAl alloys in the KState. Met. Sci. J. 4, 47–52.

Weatherly, G.C., 1975. The stability of eutectic microstructures at elevated temperatures. In: Treatise on Material Science and Technology, Vol. 8. Academic Press, New York, pp. 121–175.

Weng, K., Mao, H.K., Bell, P.M., 1982. Lattice parameters of the perovskite phase in the system $MgSiO_3$–$CaSiO_3$–Al_2O_3. Year Book Carnegie Inst. Wash. 81, 273–277.

Whiting, M.J., Tsakiropoulos, P., 1997. Morphological evolution of lamellar structures The Cu–Al eutectoid. Acta Mater. 45, 2027–2042.

Wood, B.J., 2000. Phase transformations and partitioning relations in peridotite under lower mantle conditions. Earth Planet. Sci. Lett. 174, 341–354.

Yamazaki, D., Kato, T., Ohtani, E., Toriumi, M., 1996. Grain growth rates of $MgSiO_3$-perovskite and periclase under lower mantle conditions. Science 274, 2052–2054.

Yamazaki, D., Kato, T., Yurimoto, H., Ohtani, E., Toriumi, M., 2000. Silicon self-diffusion in $MgSiO_3$-perovskite at 25 GPa. Phys. Earth Planet. Inter. 119, 299–309.